Magnetotransport properties of alkali metal doped La–Ca–Mn–O system under pulsed magnetic field: Decrease of small polaron coupling constant and melting of polarons in the high temperature phase

Sayani Bhattacharya, S. Pal, Aritra Banerjee, H. D. Yang, and B. K. Chaudhuri

Citation: J. Chem. Phys. **119**, 3972 (2003); doi: 10.1063/1.1582433
View online: http://dx.doi.org/10.1063/1.1582433
View Table of Contents: http://jcp.aip.org/resource/1/JCPSA6/v119/i7
Published by the AIP Publishing LLC.

Magnetotransport properties of alkali metal doped La–Ca–Mn–O system under pulsed magnetic field: Decrease of small polaron coupling constant and melting of polarons in the high temperature phase

Sayani Bhattacharya,[a] S. Pal, and Aritra Banerjee
Department of Solid State Physics, Indian Association for the Cultivation of Science, Kolkata-700032, India

H. D. Yang
Department of Physics, National Sun Yat Sen University, Kaohsiung-804, Taiwan, Republic of China

B. K. Chaudhuri
Department of Solid State Physics, Indian Association for the Cultivation of Science, Kolkata-700032, India and Department of Physics, National Sun Yat Sen University, Kaohsiung-804, Taiwan, Republic of China

(Received 4 November 2002; accepted 22 April 2003)

Pulsed magnetic field (0–4.4 T) was used to study the magnetic field dependent resistivity (12–350 K) and thermoelectric power (0–1.5 T) of Na and K-doped $La_{0.7}Ca_{0.7-y}A_yMnO_3$ ($0.0 \leqslant y \leqslant 0.3$, A=Na, K) system showing semiconducting to metallic transitions around temperature T_p. Na/K-doping increases both conductivity and T_p. In $La_{1-x}Ca_xMnO_3$, an increase of T_p and conductivity with an increase of Ca (for $x \leqslant 0.33$) are small and the small polaron coupling constant (γ) and hence the electron-lattice (phonon) interaction is strong. But in the Na/K doped system, γ is small and for $y \geqslant 0.05$, Motts' condition of strong el–ph interaction breaks down in the high temperature ($T > T_p$) phase. Increase of conductivity in the Na/K doped system is caused by the decrease of γ, binding energy (W_p), hopping energy (W_H), and effective mass (m_p) of the polarons leading to the melting (we call it) of polarons in the $T > T_p$ phase. This melting results in an increase of exchange coupling constant between spins. Field dependent thermoelectric power (TEP) of the samples (measured between 80–300 K) also supports the small polaron hopping conduction. The resistivity data are well fitted with the variable range hopping model for a limited range of temperature ($T_p < T < \theta_D/2$, θ_D being the Debye temperature) while thermally activated small polaron hopping model is found valid for $T > \theta_D/2$. With the application of a magnetic field, the density of states at the Fermi level increases. The TEP data indicate the importance of electron-magnon contribution in the low temperature ($T < T_p$) ferromagnetic metallic phase. Estimated polaron bandwidth (J) satisfies Holstein's condition of the adiabatic ''small polaron'' hopping conduction mechanism for the region $T > T_p$. © *2003 American Institute of Physics.* [DOI: 10.1063/1.1582433]

I. INTRODUCTION

Rare-earth manganites of the type $Ln_{1-x}M_xMnO_3$ (Ln =La, Pr, Nd, etc. and M=Ca, Pb, Ba, etc.) have attracted the attention of many researchers worldwide because of their interesting properties[1] like metal–insulator transition (MIT), ferromagnetic (FM) to paramagnetic (PM) phase change, charge ordering (CO), colossal magnetoresistance (CMR), etc. These ceramic oxide materials also show[2] a systematic variation in thermoelectric power (Seebeck coefficient) depending on the temperature as well as on the doping concentrations (x). The conduction mechanism in these mixed valence manganites is a complex interplay between magnetic spin, charge ordering and also structural change. When La^{3+} in the parent insulating $LaMnO_3$ is substituted by a divalent element (M), some of the Mn ions change its valence state from 3+ to 4+ and becomes ferromagnetic with a well-defined Curie temperature (T_c) below which the material is metallic. According to Zener,[3] magnetism in such systems is primarily caused by the double exchange (DE) mechanism which involves the hopping of a d-hole from Mn^{4+} ($d^3, t_{2g}^3, S=3/2$) to Mn^{3+} ($d^4, t_{2g}^3, e_g^1, S=2$) via the central oxygen atom. Recently, several theoretical and experimental[4] investigations indicate that in addition to the DE interaction, a second mechanism such as the formation of small polarons in the paramagnetic (semiconducting) phase ($T > T_p$) should be invoked in order to explain the basic physics of doped manganites. A strong electron (hole)-lattice (phonon) interaction involved in such compounds leads to the polaron formation[5] and polaronic hopping conduction mechanism has been used to explain the semiconducting behavior above T_p. Recently, some reports of correlated polaron (bipolarons) formation have also been reported.[6] However, there is no consensus[7] about the bipolarons (or two small polarons) at the elevated temperatures ($T > T_p$). So far, variable range hopping (VRH) model has been used to explain[8,9] the conductivity data above T_p. However, controversy still exists whether this model could be used for the entire temperature above MIT or not. The VRH model is, in general, applicable for the low temperature region well below the Debye temperature. It has also been shown in a

[a]Author to whom correspondence should be addressed. Electronic mail: sspsb2@mahendra.iacs.res.in; Fax: +91-33-4732805.

recent paper[10] that the VRH model is valid for the La–Pb–Mn–O-type system for a limited range of temperature ($T_p < T < \theta_D/2$). Application of this model for the manganite system in the high temperature range (well above T_p) has not yet been well studied. Thus it is necessary to further study the conductivity data of different samples using this model.

For such an investigation, we have prepared a new alkali metal doped system where both monovalent alkali ion substitutions in the Ca site in La–Ca–Mn–O and application of magnetic field causes large increase of conductivity and MIT temperature T_p. Polaron coupling constant (γ) and other related parameters describing small polaron hopping conduction also decrease. In recent years, there are only a few reports[11–14] of transport measurements on monovalent alkali-metal ion doped compounds (in the La site only) like La–Na–Mn–O, La–K–Mn–O, and La–Sr–Na–Mn–O. But there is no consensus on the effect of Na doping on T_p and transport properties. Furthermore, recently Zouari *et al.*[15] observed no MIT in the Na, K doped $Pr_{0.8}Na_{1-x}K_xMnO_3$ system. All these prompted us to study the effect of monovalent alkali (Na) substitution in the Ca-site of La–Ca–Mn–O manganite. It is also worth mentioning that conductivity, magnetoresistance, and thermoelectric power (Seebeck coefficient) of the CMR materials have been measured, so far, mostly under continuous dc magnetic field.[16] In the present study we have used a pulsed magnetic field of short duration to study the transport properties (magnetoresistance) of the selected sample giving identical results as those obtained under dc magnetic field. Obviously, the advantage of the pulsed field is a high field of short duration, using relatively easy process, for studying magnetic properties of solid samples. Moreover, as the field is produced for an extremely short period, the heating effect is not very pronounced. So, in the present work, pulsed magnetic field[17] (0–4.4 T) has been applied to study the temperature and magnetic field dependent resistivity and TEP (at 0 and 1.5 T field) of Na/K doped $La_{1-x}Ca_{x-y}A_yMnO_3$ (A=Na and K) for all the samples (with $x=0.3$, $0.0 \leqslant y \leqslant 0.3$). Since both Na and K doped samples show the same thermal variation of resistivity and TEP data and identical theoretical analysis is valid for all the samples, we concentrate our discussion on the Na doped samples only. Moreover, since TEP has been measured at 0 and 1.5 T magnetic field, resistivity data are shown only at 0 and 1.5 T magnetic field. The change (decrease) of maximum resistivity (ρ_{max}) with an increase of field (0–4.4 T) has, however, been shown in this paper. From the study of field dependent resistivity (ρ) and thermoelectric power (S), we tried to find the effect of magnetic field on the polaron coupling constant (γ) which is a measure of the electron-lattice (phonon) interaction constant, the nature of hopping (adiabatic or nonadiabatic), DOS at the Fermi level [$N(E_F)$], polaron hopping energy (W_H), polaron effective mass (m_p), polaron band width (J), etc. All these parameters indicated in favor of the presence of small polarons in the system of our investigation. Present study also points out the breaking of the Mott's condition[18] of strong el–ph interaction ($\gamma > 4$) in the present system with the increase of Na/K concentration (for $y > 0.05$). The corresponding decrease in the polaron binding energy and hopping energy leads to the melting of the small polaron in the high temperature ($T > T_p$) phase instead of forming large polarons.

II. EXPERIMENT

$La_{1-x}Ca_{x-y}Na_yMnO_3$ (with $x=0.3$ and $y=0.0$, 0.05, 0.1, 0.15, 0.3) of our present investigation were prepared by a standard ceramic processing technique similar to our earlier work.[17] Well mixed stoichiometric mixtures of La_2O_3, CaO, Na_2CO_3, and $(CH_3COO)_2Mn, 4H_2O$ each of purity 99.99% were first heated to 773 K and then to 1073 K for 5 h with intermediate grinding and then again annealing at 1173 K for 48 h. The sintered powder thus obtained was ground, palletized and annealed again at 1073 K for 72 h and then furnace cooled. For the K doped sample K_2CO_3 was taken instead of Na_2CO_3 and similar heating procedure were followed. X-ray powder diffraction study made with Cu K_α radiation shows single-phase character of all the samples. Crystallographic structure of the sample with $y=0.0$ is indexed as orthorhombic one, while the doped samples (with $y=0.05$, 0.1, 0.15, and 0.3) can be indexed by a rhombohedral lattice, which is consistent with the previously reported results.[11,12] The resistivity and thermoelectric power of the samples were measured in the temperature range 12–350 K and 80–300 K, respectively, with an accuracy of temperature measurement ± 0.5 K. For the measurement of magnetoresistance under pulsed field, we used a lab-made setup of a pulsed magnetic field produced in an air-core solenoid coil by sudden discharge of a capacitor bank and the data were stored in a digital storage oscilloscope (Iwatsu, DS-6612, 60 MHz). The sample was mounted on the tail-end part of the modified closed cycle helium cryostat (Displex, Air Products) made by attaching a copper rod onto the lower part of the original displex. The sample placed nearly at the center of the solenoid coil feels a pulsed magnetic field in a vertical direction whenever a surge of current passes through the coil. Varying the capacitor voltage with the help of a variac changes the strength of the magnetic field. In the present case, we have measured upto a maximum magnetic field of 4.4 T. Detailed method of measurement of magnetic field has been discussed elsewhere.[17] The thermoelectric power (S) was measured by the standard differential technique in the 80–300 K temperature ranges. All the experimental data were collected in the heating direction after confirming the steady state. The temperature difference between the two electrodes (ΔT) was maintained around 2 K with a programmable current source (Keithley 220). A Keithley 181 nanovoltmeter recorded the thermo-emf (ΔV) developed between the two surfaces of the sample and the temperature difference (ΔT) and thermopower was calculated from the relation $S=\Delta V/\Delta T$. A K-type (chromel-alumel) thermocouple (corrected) was used for temperature measurement with a WAHL data scanner (Model DS62) with an accuracy of ± 0.1 K.

III. RESULTS AND DISCUSSION

A. Magnetic field dependent conductivity mechanism (above and below T_p)

The thermal variation of the electrical resistivity (between 12–350 K) of the Na doped $La_{0.7}Ca_{0.3-y}Na_yMnO_3$

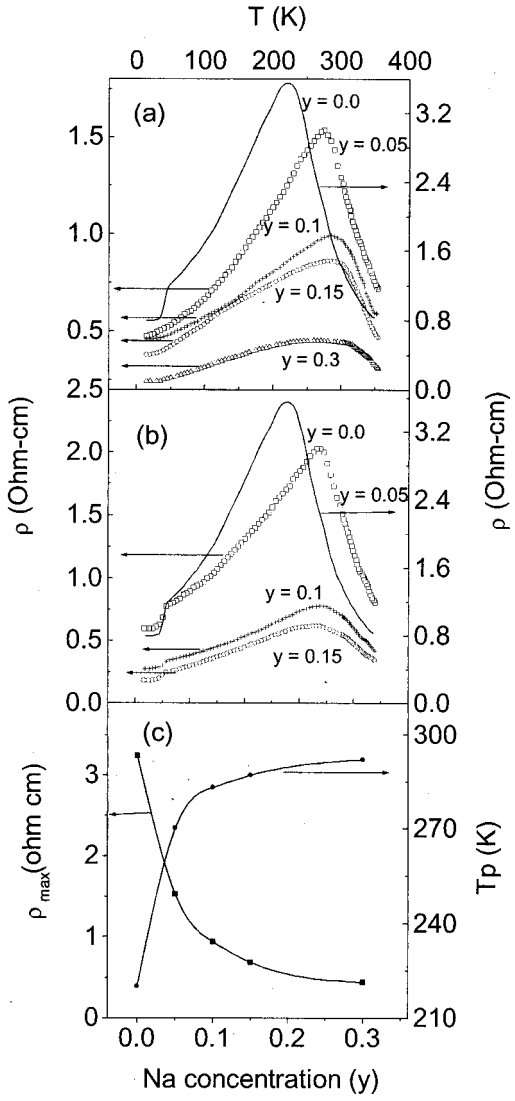

FIG. 1. Thermal variation of resistivity (ρ) of (a) $La_{0.7}Ca_{0.3-y}Na_yMnO_3$ ($0.0 \leqslant y \leqslant 0.3$) and (b) $La_{0.7}Ca_{0.3-y}K_yMnO_3$ ($0.0 \leqslant y \leqslant 0.15$) at zero applied field. (c) Maximum resistivity (ρ_{max}) and metal insulator transition (MIT) temperature T_p as a function of doping concentration (y) showing clearly the saturation of ρ_{max} and T_p after a certain doping level.

with different doping concentration (y) shown in Fig. 1(a). The corresponding curve for the K doped samples shown in Fig. 1(b) indicates identical behavior with that of the Na doped samples. For all the Na/K doped samples, distinct peaks are observed in the resistivity versus temperature

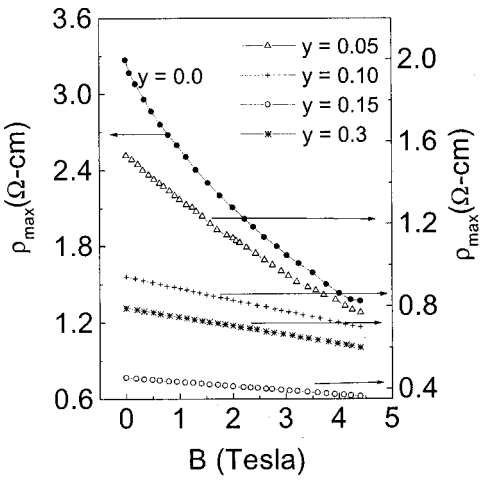

FIG. 2. Variation of maximum resistivity (ρ_{max}) at the metal insulator transition temperature (T_p) of the $La_{0.7}Ca_{0.3-y}Na_yMnO_3$ ($0.0 \leqslant y \leqslant 0.3$) samples with an increase of magnetic field ($B = 0-4.4$ T).

curves around T_p. The T_p values of the samples are obtained from the curves in Fig. 1, where $d\rho/dT = 0$. The low temperature ($T < T_p$) resistivity shows metallic behavior with $d\rho/dT > 0$. The maximum resistivity ρ_{max} (peak value) decreases and T_p shifts to the higher temperature as Na or K concentration y increases (Table I). This increase in conductivity with Na/K doping is considered to be associated with the increase of the ratio of Mn^{4+}/Mn^{3+}, which in turn contributes to the enhancement of hole concentration in the e_g band. The values of the ratio of Mn^{4+}/Mn^{3+} with increasing y, obtained from the valency calculations (Table I) supports this argument. The cation valency distribution can be represented as $La^{3+}_{1-x}Ca^{2+}_{x-y}Na_y[Mn^{3+}_{1-(x+y)}Mn^{4+}_{x+y}]O_3$. For every y amount of Na^+ or K^+ ions, there is an increase of $(x+y)$ amount of Mn^{4+} ions. Hence, even for a small amount of Na/K doping, there will be a huge increase of charge carriers and thus resistivity is decreased with increase of Na/K concentration. Moreover, with the increase in the ratio of Mn^{4+}/Mn^{3+}, the ferromagnetic double-exchange (FMDE) interaction increases and, therefore, the extension of metallic phase is obtained with increasing Na/K doping. After a certain optimal amount of doping concentration (y) when there is sufficient Mn^{4+} ions, superexchange interaction through the π orbital, $t_{2g}(Mn)-2p_\pi(O)-t_{2g}(Mn)$ dominates over the DE interaction and hence T_p almost saturates [as observed from Fig. 1(c)]. Figure 2 shows the shifting of maximum resistivity (ρ_{max}) at T_p (obtained from the

TABLE I. Room temperature resistivity (ρ_{RT}), metal–insulator (MIT) transition temperature (T_p), Debye temperature (θ_D), Mn^{4+}/Mn^{3+} ratio, and some other important estimated parameters of $La_{0.7}Ca_{0.3-y}Na_yMnO_3$ for different values of Na ion concentration (y).

y	r_p (Å)	m_p (g) $\times 10^{25}$	R (Å)	N (cm^{-3}) $\times 10^{-21}$	θ_D (K)	ν_{ph} (Hz) $\times 10^{-13}$	ρ_{RT} (ohm cm)	T_p (K)	Mn^{4+}/Mn^{3+}
0.0	1.63	5.2649	4.04	15.208	510.20±1	1.063	1.44±0.05	220±1	0.428
0.05	1.67	1.7163	4.16	13.908	569.80±1	1.187	1.31±0.05	270±1	0.538
0.10	1.60	0.9648	3.97	16.024	626.96±1	1.306	0.91±0.05	283±1	0.666
0.15	1.60	0.6662	4.00	15.997	653.59±1	1.361	0.67±0.05	287±1	0.818
0.30	1.70	0.4772	4.22	13.261	657.90±1	1.370	0.44±0.05	292±1	1.500

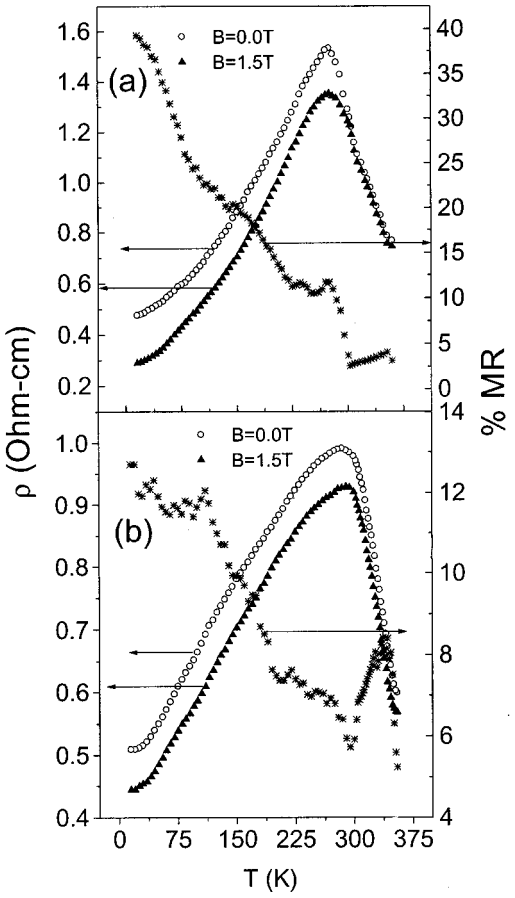

FIG. 3. Variation of resistivity in the absence ($B=0.0$ T) and presence ($B=1.5$ T) of the magnetic field (B) and %MR (for $B=1.5$ T) with temperature for the sample $La_{0.7}Ca_{0.3-y}Na_yMnO_3$ with $y=$ (a) 0.05 and (b) 0.15.

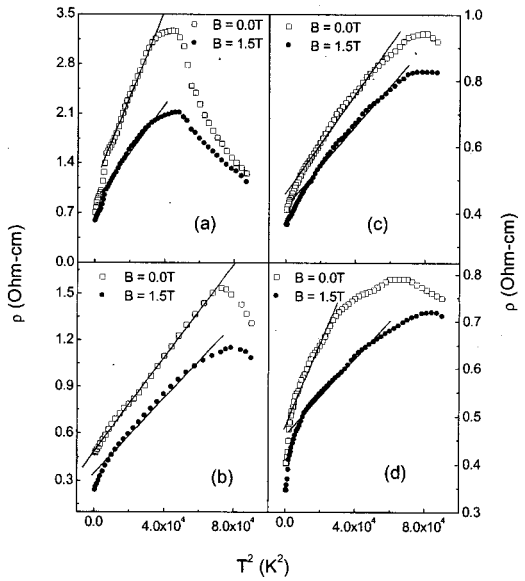

FIG. 4. Linear fit of the low temperature (low temperature $T<T_p$ FM region) resistivity data with the T^2 term [Eq. (1)] in the absence ($B=0$) and presence ($B=1.5$ T) of the magnetic field (B) for the samples $La_{0.7}Ca_{0.3-y}Na_yMnO_3$ with (a) $y=0.0$, (b) $y=0.05$, (c) $y=0.1$, (d) $y=0.15$.

study of field dependent resistivity of the samples) towards lower resistivity value with an increase of magnetic field (from 0 to 4.4 T). For the Na doped sample in the La site viz., $La_{1-x}Na_xMnO_3$, Rao *et al.*[12] and Roy *et al.*[14] also obtained similar results where increasing Na content results in an increase in conductivity and T_p. On the contrary, for the $La_{0.7}Sr_{0.3-x}Na_xMnO_3$ system Abdelmoula *et al.*[13] reported an increase in ρ and decrease of T_p with increasing Na content which they attributed to the weak DE interaction and smaller M-site cation radius $\langle r_M \rangle$.

We notice from Fig. 3 that the application of magnetic field decreases the resistivity of the Na doped $La_{0.7}Ca_{0.3-y}Na_yMnO_3$ oxides throughout the temperature range of our investigation and T_p shifts towards higher temperature side. Similar is the case with the K doped samples. This observation may be explained by considering that with the application of a magnetic field, local ordering of magnetic spin occurs which causes the ferromagnetic metallic (FMM) state to suppress the paramagnetic insulating (PMI) state and, therefore, T_p shifts towards higher temperature. Because of the spin ordering, the charge carriers also suffer less scattering with the increase of exchange interaction and hence resistivity decreases thereby showing a large negative magnetoresistance (MR) $[-(R_H-R_0)/R_0\times 100\%$, where R_H and R_0 are, respectively, the resistances in presence and in absence of magnetic fields]. As the spin ordering is more pronounced in the low temperature FM phase, the effect of magnetic field on resistivity is more in this low temperature phase whereas in the PMI state ($T>T_p$), the effect of field on the resistivity is comparatively smaller. The decrease in resistivity, due to applied field, is maximum near the resistivity peak thereby showing a peak in the %MR versus temperature plot (Fig. 3) around T_p.

As observed from Fig. 4, the resistivity data for all the samples in the low temperature FM phase can be fitted with an equation of the form,

$$\rho=\rho_0+\rho_2T^2, \tag{1}$$

where the temperature independent part ρ_0 is the resistivity due to domain, grain boundary and other temperature independent scattering mechanism. The second term was described by Urushibara *et al.*[1] as arising from electron–electron scattering process dominating the low temperature transport phenomenon. But due to Mott,[19] a $\rho\sim T^2$ term does not necessarily suggest only electron–electron scattering and he further recommended that electron–magnon scattering must be associated with the resistivity in the FM phases. The parameters obtained from best fitting of the low temperature resistivity data with Eq. (1) are shown in Table II. It is seen that ρ_0 decreases significantly with magnetic field due to the influence of the magnetic field on the magnetic domains. As magnetic field increases, domain boundary decreases and hence ρ_0 becomes smaller.[10,20] The decrease in the electron-spin scattering term ρ_2 is considered to be due to the suppression of spin fluctuation in presence of magnetic field (proportional to $H^{-1/3}$).[21]

Again, in the high temperature ($T>T_p$) insulating (semiconducting) phase, the conductivity data dominated by

TABLE II. The values of the parameters ρ_0 and ρ_2 obtained from fitting the low temperature ($T<T_p$) resistivity data with Eq. (1) both in the presence ($B=1.5$ T) and in the absence ($B=0$) of the magnetic field B for the $La_{0.7}Ca_{0.3-y}Na_yMnO_3$ for different values of Na concentration (y).

	ρ_0 (Ohm cm)		ρ_2 (Ohm cm K^{-2})	
y	$B=0.0$ T	$B=1.5$ T	$B=0.0$ T	$B=1.5$ T
0.0	1.13	0.97	6.10×10^{-5}	3.40×10^{-5}
0.05	0.48	0.45	1.52×10^{-5}	1.28×10^{-5}
0.10	0.46	0.42	7.25×10^{-6}	6.06×10^{-6}
0.15	0.45	0.45	6.07×10^{-6}	4.53×10^{-6}
0.30	0.26	0.24	4.90×10^{-6}	4.49×10^{-6}

the thermally activated hopping of a small polaron[22] are fitted well with the small polaron hopping (SPH) model of Mott[23] viz.,

$$\rho/T=\rho_\alpha \exp(E_p/k_BT), \tag{2}$$

where $\rho_\alpha=[k_B/\nu_{\rm ph}Ne^2R^2C(1-C)]\exp(2\alpha R)$, k_B is the Boltzmann constant, and T is the absolute temperature. N is the number of ion sites per unit volume (obtained from the density data), R is the average intersite spacing obtained from the relation $R=(1/N)^{1/3}$, C is the fraction of sites occupied by a polaron, α is the electron wave function decay constant obtained from fitting the experimental conductivity data, $\nu_{\rm ph}$ is the optical phonon frequency (estimated from the relation $h\nu_{\rm ph}=k_B\theta_D$, the Debye temperature θ_D is estimated from the conductivity data). The estimated values of optical phonon frequency (Table I) are found to be very close to the $\nu_{\rm ph}$ value estimated from the infrared spectra (Fig. 5, corresponding to the peak at nearly 600 cm^{-1}) which is of the order of 1.28×10^{13} Hz. Thus the optical phonon frequency does not change appreciably in these samples. The activation energy (E_p) for hopping conduction is given by $E_p=W_H+W_D/2$ (for $T>\theta_D/2$) (where $E_p=W_D$ for $T<\theta_D/4$, W_H is the polaron hopping energy and W_D is the disorder energy). The calculated values of R are shown in Table I. The difference between the E_p and E_s (activation energy estimated from the high temperature TEP data discussed below) is the polaron hopping energy. Therefore, W_H is estimated from the relation $W_H=E_p-E_S$. In Fig. 6 we plotted the resistivity curve as $\ln(\rho/T)$ versus $1/T$ and from the slope of this curve above $\theta_D/2$, we have estimated the activation energy E_p. The values of $\theta_D/2$ are obtained from the temperature where the linearity disappears in the high temperature region. From the values of E_p and E_S shown in Table III, we see that with

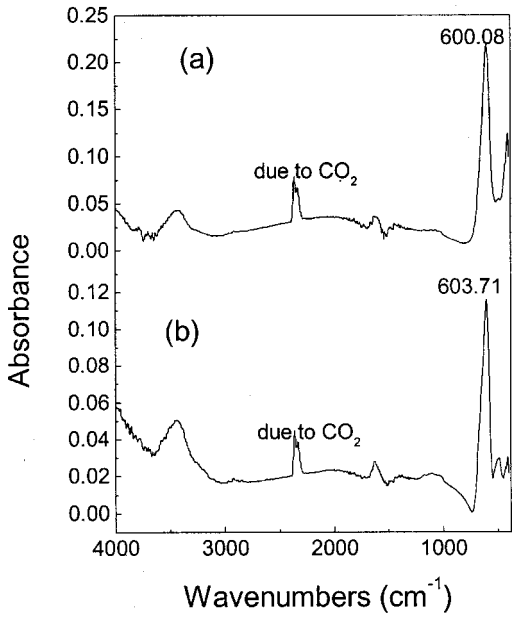

FIG. 5. Infrared spectra of two typical samples $La_{0.7}Ca_{0.3-y}Na_yMnO_3$ with (a) $y=0.0$ and (b) $y=0.1$ in the KBr pellet at room temperatures from where optical phonon frequency was estimated and compared with that obtained from the conductivity data (from Debye temperature).

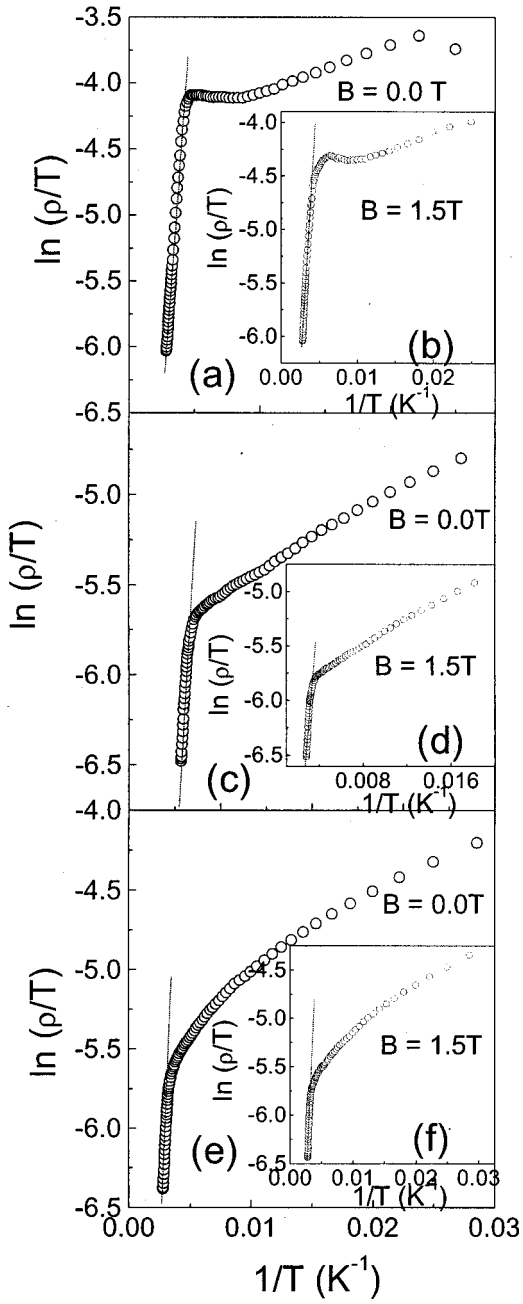

FIG. 6. Variation of $\ln(\rho/T)$ as a function of inverse temperature $1/T$ for the sample $La_{0.7}Ca_{0.3-y}Na_yMnO_3$ with $y=0.0$ for (a) and (b); $y=0.10$ for (c) and (d); $y=0.15$ for (e) and (f). Inset graphs (b), (d), and (f) shows the plot with field $B=1.5$ T. Solid lines are the best fit to the SPH model [Eq. (2)].

TABLE III. The values of activation energies estimated from conductivity (E_p) and thermoelectric power (E_S) data and polaron hopping energy (W_H) of $La_{0.7}Ca_{0.3-y}Na_yMnO_3$ for different values of y in the presence ($B=1.5$) and absence ($B=0$) of the magnetic field (B). The estimated values of dielectric constant (ϵ) and small polaron coupling constant (γ) are also shown for different samples.

	E_p (meV)		E_S (meV)		W_H (meV)		ϵ		$\gamma=2W_H/h\nu_{ph}$	
y	$B=0.0$ T	1.5 T	0.0 T	1.5 T	0.0 T	1.5 T	0.0 T	1.5 T	0.0 T	1.5 T
0.0	116.33	91.95	13.16	9.38	103.17	82.57	12.81	16.01	4.69	3.75
0.05	104.59	83.87	12.76	11.34	91.84	72.53	13.97	17.69	3.74	2.95
0.10	97.31	79.22	11.79	10.93	85.52	68.29	15.73	19.7	3.16	2.52
0.15	91.92	77.20	11.60	9.64	80.31	67.56	16.83	20.01	2.85	2.39
0.30	85.29	75.06	10.69	9.38	74.60	65.68	16.93	19.23	2.63	2.31

increasing value of sodium concentration (y), both the activation energies gradually decrease. This behavior is explained by considering that increasing y causes charge delocalization (due to decrease of γ or el–ph interaction constant) in the system and thereby the energy required to liberate a free carrier is reduced. We have also calculated the magnetic field dependent activation energies and observed that with the application of field, activation energy decreases for every doping concentration of Na (y) (Table III). This is due to delocalization of charge carriers reported earlier[17] and spin ordering in the system.

As mentioned earlier in this paper and also reported in our previous work[17] that the low temperature ($T<\theta_D/2$) transport phenomenon in perovskites and in some other semiconducting oxides are described by variable range hopping (VRH) of the charge carriers. Recently Jaime *et al.*[8] and Viret *et al.*[9] applied VRH conduction mechanism in the La–Ca–Mn–O system for the entire temperature above T_p. But as reported earlier,[5] the VRH model was derived for explaining the conductivity data below $\theta_D/2$. Conductivity data of the present samples are also best fitted with the VRH model between T_p and $\theta_D/2$ and above $\theta_D/2$, small polaron hopping (SPH) model was applicable as discussed earlier. The expression for conductivity in the VRH model has the form $\sigma_{dc}=\sigma_0\exp(-T_0/T)^{1/4}$, where T_0 is a constant $[=16\alpha^3/k_BN(E_F)]$ and $N(E_F)$ is the density of states (DOS) at the Fermi level which is calculated from the slope of the $\log\sigma_{dc}$ versus $T^{-1/4}$ curves (Fig. 7). The calculated values of $N(E_F)$ both in absence ($B=0$) and in presence of magnetic field are shown in Table IV. To calculate the values of $N(E_F)$, we have used $\alpha=2.22$ nm^{-1} (similar to the value used by Viret *et al.* for La–Sr–Mn–O samples) and T_0 is found to be $\sim 10^6$. $N(E_F)$ values are also in good agreement with the previously reported values.[5] It is noticed from these estimated values that $N(E_F)$ increases with increasing Na concentration (y). Application of magnetic field also increases $N(E_F)$ for all Na concentrations. This increase of $N(E_F)$ with the increase of both by Na doing and field is also expected, as the increase in conductivity is the obvious effect of the increased number of charges at the Fermi level.

Next, we tried to find out the nature of hopping conduction mechanism (adiabatic or nonadiabatic) both in presence and in absence of magnetic fields. It is recognized[23] that when the polaron band width $J[=J_0\exp(-2R\alpha)]$ approaches J_0, the hopping is adiabatic and the conduction is mainly controlled by the activation energy. Now, according

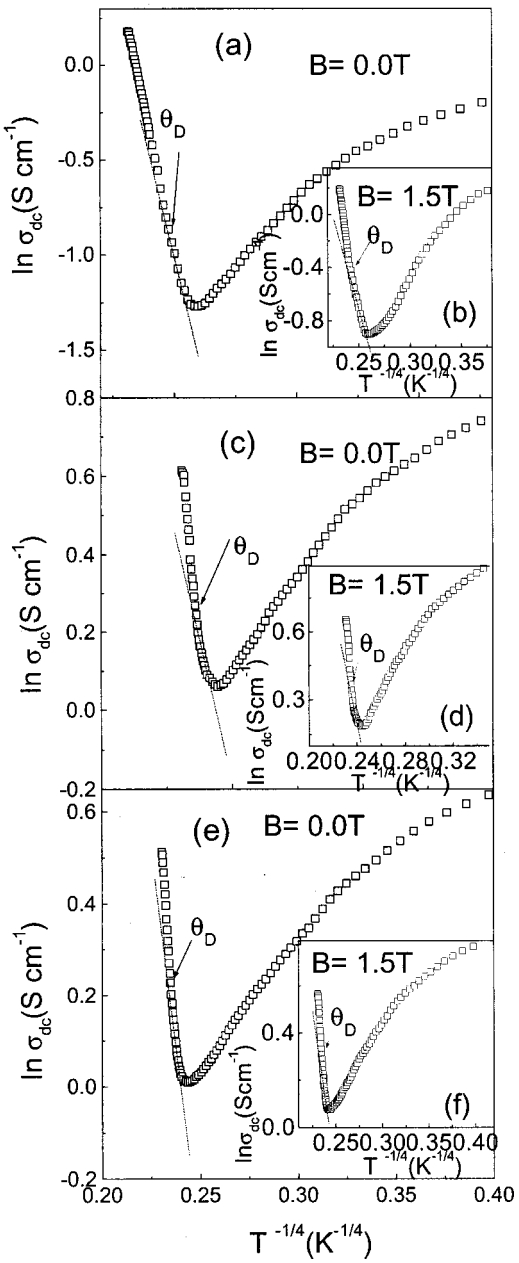

FIG. 7. Plot of $\log\sigma_{dc}$ as a function of $T^{-1/4}$ for the sample $La_{0.7}Ca_{0.3-y}Na_yMnO_3$ with $y=0.0$ for (a) and (b); $y=0.10$ for (c) and (d); $y=0.15$ for (e) and (f). Inset graphs (b), (d), and (f) show the plot with field $B=1.5$ T. Solid lines are the best fit to the VRH model $[\sigma_{dc}=\sigma_0\exp(-T_0/T)^{1/4}]$ between T_p and $\theta_D/2$, where θ_D is the Debye temperature.

TABLE IV. Values of the density of states (DOS) at the Fermi level $N(E_F)$, polaron bandwidth (J), and λ in the presence ($B=1.5$ T) and absence ($B=0$) of the magnetic field (B) estimated for different concentrations (y) for the sample $La_{0.7}Ca_{0.3-y}Na_yMnO_3$ undergoing metallic transition at T_p.

	$N(E_F)$ (eV^{-1} cm^{-3})$\times 10^{-20}$		W_p (meV)		J (eV)		λ (eV)		α'	
y	$B=0.0$ T	1.5 T	0.0 T	1.5 T	0.0 T	1.5 T	0.0 T	1.5 T	0.0 T	1.5 T
0.0	3.8	17.9	262.54	218.54	0.0281	0.0267	0.0240	0.0227	−0.61	−0.4
0.05	6.938	7.153	238.67	193.05	0.0275	0.0240	0.0246	0.0232	−0.52	−0.3
0.10	8.521	8.783	224.04	180.98	0.0265	0.0222	0.0254	0.0220	−0.47	−0.3
0.15	10.062	10.964	212.82	179.52	0.0261	0.0222	0.0255	0.0219	−0.41	−0.3
0.3	12.998	13.571	197.80	174.76	0.0243	0.0217	0.0241	0.0212	−0.34	−0.2

to Holstein's condition[24] applicable for small polaronic conduction, the polaron bandwidth J should satisfy the inequality $J>\lambda$ (for adiabatic hopping) and $J<\lambda$ (for nonadiabatic hopping) where $\lambda=(2k_BTW_H/\pi)^{1/4}(h\nu_{ph}/\pi)^{1/2}$. In calculating λ values we have used previously calculated W_H (Table III) and ν_{ph} (Table I) values. The J is independently calculated from the model proposed by Mott and Davis[23] viz., $J\sim e^3[N(E_F)/\epsilon^3]^{1/2}$ where the high frequency dielectric constant of the sample ϵ is calculated from the relation $W_H=e^2/4\epsilon(1/r_p-1/R)$ and r_p is the polaron radius [estimated from the relation $r_p=1/2(\pi/6N)^{1/3}$]. Average dielectric constant estimated from the reflectance spectra by Mayr *et al.*[25] for the sample $La_{0.875}Sr_{0.125}MnO_3$ shows that for frequencies below phonon modes, dielectric constant (ϵ) is dominated by a large static value amounts to 60 at low temperatures and it decreases to a value 30 at room temperatures. They assigned it to the increase in permeability in FM phase. In the vibrational frequency regime, via ionic polarizability, ϵ is reduced to values close to 10. They explained the dielectric loss at low frequencies to be dominated by hopping process of charge carriers strongly coupled to the lattice that are thermally excited, resulting in a strong temperature and frequency dependence. The ϵ value estimated from our data in the high temperature regime also shows a value ~10. Exploiting the values of $N(E_F)$ (Table IV) and ϵ (Table III), the estimated J values (given in Table IV) indicate that J decrease with increasing doping concentration of Na. The inequality $J>\lambda$ is well satisfied for all the samples suggesting adiabatic hopping conduction mechanism both in presence and in absence of magnetic field. Here it should be mentioned that the condition for small polaron formation given by $J\leqslant W_H/3$ (Tables III and IV) and $r_p<R$ (Table I) is well satisfied for our samples both in presence and in absence of field further asserting the presence of small polaron in the present system.

To estimate the small polaron coupling constant (γ), which is also a measure of the el–ph interaction constant of the sample, the relation due to Mott[18] viz., $\gamma=2W_H/h\nu_{ph}$ is used. Millis *et al.*[26] have revealed that γ is a crucial parameter controlling the Curie temperature T_c which is close to the MIT temperature T_p for the present system. In Table III, the estimated values of γ show that with increasing y, γ decreases and thereby an increase of T_p is obtained, which is in agreement with the theory proposed by Millis *et al.* With the application of magnetic field, γ decreases, as predicted, showing decrease in el–ph coupling due to application of magnetic field (and hence causing an increase of conductivity). For the La–Na–Mn–O system showing an increase of T_p with Na doping, Rao *et al.*[12] predicted that Na doping induces a transition from strong Hund coupling between e_g and t_{2g} spins to weak Hund coupling. In addition, they argued that MIT corresponds to a transition from a strong el–ph coupling, giving rise to a high resistivity, to a weak el–ph coupling that favors low resistivity. From the calculation of the coupling constant γ, we confirmed that increase of T_p with Na doping is associated with the decrease of γ. We also estimated the polaron binding energy W_p (Table IV) and effective mass m_p (Table I) of the polarons in the high temperature ($T>T_p$) phase from the following relations:[27] $W_H=W_p/2-J$ and $m_p=[\hbar/2\omega_0R^2]\exp(\gamma)$ for adiabatic hopping ($\omega_0=2\pi\nu_{ph}$). Since the values of R and phonon frequency ν_{ph} (Table I) are almost constant for all the samples, the effective mass of the polaron decreases with an increase of y and magnetic field or with the increase of conductivity of the samples. So the decrease of all the parameters W_H, W_p, polaron coupling constant and m_p do not indicate that small polarons become large polarons (or bipolarons) in the high temperature phase ($T>T_p$) as reported in some recent work.[6] Effective mass of small polarons is much lower than that of bipolarons[28] with lower mobility and hence lower conductivity. Further support of the small polaron will be obtained from the high temperature TEP data discussed below. Actually, small polarons are slowly melted with the reduction of W_P as mentioned above, which results in the increase of spin–spin and electron–spin interaction. Using the parameters already derived, we find that the values of both polaron binding energy and effective mass reduce with the application of magnetic field and increase of the Na/K content. This destabilizes the small polarons which was also recently pointed out by Egami *et al.*[7,29] From the present study we find that this small polaron instability may occur by doping as well as by increasing the magnetic field which enhances conductivity.

Therefore, the addition of Na/K leads the present system of our investigation from the polaronic hopping conduction regime towards the regime where conduction mechanism is governed by electron and spins. This is unlike the case of some high T_C cuprates showing semiconducting to superconducting transition where spin contribution to the conduction (above T_C) is not present or negligible. It has been shown theoretically by Mott[18] that a larger value of $\gamma>4$ indicates strong el–ph interaction as observed in insulating (semicon-

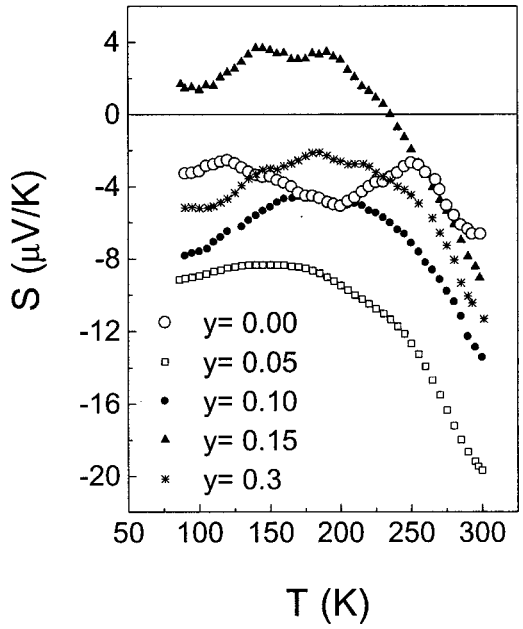

FIG. 8. Thermal variation of the Seebeck coefficient (S) of $La_{0.7}Ca_{0.3-y}Na_yMnO_3$ with $y=0$, 0.05, 0.1, 0.15, and 0.3 without applying the magnetic field.

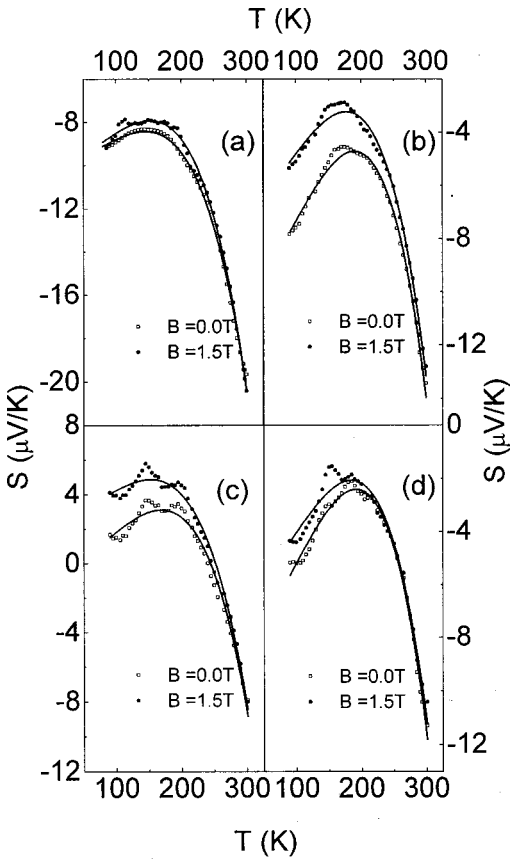

FIG. 9. Temperature and magnetic field ($B=1.5$ T) dependent Seebeck coefficient (S) of four different samples $La_{0.7}Ca_{0.3-y}Na_yMnO_3$ with (a) $y=0.05$, (b) 0.1, (c) 0.15, and (d) 0.3. Solid lines are best fit lines to Eq. (3).

ducting) samples like $LaMnO_3$. From the estimated values of γ, we find that only for the samples with $y<0.05$, for example, $La_{0.7}Ca_{0.3}MnO_3$, the values of $\gamma>4$. With increasing y, small polaron coupling and el–ph coupling decreases and γ becomes <4 (for $y\geqslant 0.05$). This signifies that in the Na doped systems, the probability of polaron formation decreases (or delocalization occurs) as y increases and hence electronic (metallic) conduction plays a major role. The conductivity data also shows that with increasing y, conductivity increases which further specifies the decreasing of el–ph interaction. This is considered to be one of the most important effects of Na/K doping on the manganite samples. It would be worthwhile to mention here that even for the corresponding undoped $La_{1-x}Ca_xMnO_3$ system, where T_p increases with Ca content with the highest T_p for $x=0.33$, the value of the small polaron coupling constant γ does not become less than 4 in the $T>T_p$ regime which distinguishes the La–Ca–Mn–O system from the present La–(Ca–Na)–Mn–O system of our investigation. In both the cases, however, conduction is due to small polaron hopping mechanism and the conductivity data cannot be fitted with bipolaron model.[28]

B. Magnetic field dependent thermoelectric power

Magnetic field ($B=0-1.5$ T) dependent thermoelectric power (Seebeck coefficient, S) of the Na doped $La_{0.7}Ca_{0.3-y}Na_yMnO_3$ ($0.0\leqslant y\leqslant 0.3$) system measured in the temperature range 80–300 K also supports the conductivity results discussed above. Figure 8 displays the temperature dependent thermoelectric power of the samples with different values of $y=0.0$, 0.05, 0.1, 0.15, and 0.3. It is seen that for the Na free undoped sample ($y=0.0$), there is no change in sign of the Seebeck coefficient (S) and it remains negative throughout the temperature range of our investigation. It is further noticed that Seebeck coefficient becomes more negative with the addition of even a very small amount of sodium ($y=0.05$) in the Ca-site which is due to the increase of Mn^{4+} ion concentration. With further increase of y, S tends towards positive value finally becoming positive for $y=0.15$ at low temperatures. Addition of larger amount of Na ions (for $y=0.1$ and 0.15) in the M-site causes more hole doping centers which are localized in character and hence S value increases. This large value of thermopower arising from hole localization may occur due to the narrowing of e_g band (due to smaller value of M-site average radii $\langle r_M\rangle$) and it also indicates distortion of the Fermi surface. The values of S for the sample with the highest doping ($y=0.3$) and the undoped ($y=0.0$) sample are almost same (Fig. 8). This is because of the fact that for both the samples the relative % of Mn^{4+} and Mn^{3+} are nearly the same (60%–40% for $y=0.3$ and 30%–70% for $y=0.0$) and the ionic radii of Ca (0.99 Å) and Na (0.97 Å) ions are almost equal. The two factors (viz., Mn^{4+}/Mn^{3+} ratio and ionic radii), determining the sign and magnitude of S, seem to be well matched for these two concentrations.

Figure 9 shows the variation of the Seebeck coefficient S with T in the absence and in the presence of a magnetic field ($B=1.5$ T). For all the samples, it is observed that with the application of a magnetic field ($B=1.5$ T), S values increase at low temperature and the difference between the two values $\Delta S[(=S(0)-S(1.5))$, where $S(0)$ and $S(1.5)$ is the S value in the absence and presence of the 1.5 T field] decreases near

TABLE V. The values of the parameters S_0, $S_{1.5}$, and S_4 obtained from fitting the low temperature (ferromagnetic metallic phase) thermoelectric power (TEP) data of $La_{0.7}Ca_{0.3-y}Na_yMnO_3$ ($y=0-0.3$) with Eq. (4) both in the presence ($B=1.5$ T) and absence ($B=0$) of the magnetic field (B).

	S_0 (μV/K)		$S_{1.5}$ (μV/K$^{2.5}$)		S_4 (μV/K^5)	
y	$B=0.0$ T	1.5 T	$B=0.0$ T	1.5 T	$B=0.0$ T	1.5 T
0.00	−3.84	−3.71	2.34×10^{-3}	2.30×10^{-3}	-4.10×10^{-9}	-5.69×10^{-9}
0.05	−11.17	−9.93	2.27×10^{-3}	1.70×10^{-3}	-2.44×10^{-9}	-2.36×10^{-9}
0.10	−10.41	−7.39	3.42×10^{-3}	2.80×10^{-3}	-2.63×10^{-9}	-2.51×10^{-9}
0.15	1.91	2.48	2.72×10^{-3}	2.13×10^{-3}	-2.98×10^{-9}	-2.97×10^{-9}
0.30	−7.23	−6.85	3.18×10^{-3}	3.05×10^{-3}	-2.57×10^{-9}	2.47×10^{-9}

T_p. This indicates that spin ordering that occurs under magnetic field, increases the thermopower of the present manganite samples. It has previously been found[30] that phonon drag (S_g) and magnon drag (S_m) contributions are present in the low temperature region and these contributions are proportional to their respective specific heat contributions so that $S_g \alpha T^3$ and $S_m \alpha T^{3/2}$. This suggests that in the low temperature ferromagnetic phase, a magnon drag effect is produced due to the presence of electron–magnon interaction along with the effect of phonon drag due to electron–phonon interaction. But the effect of phonon drag contribution in the present sample is marginally greater than the magnon drag effect in the region of $S_{\max}$ (which is well below T_p, the MIT region). Thus, the phonon drag effect makes a major contribution in determining the low temperature peak ($S_{\max}$) of thermopower. The temperature dependence of S below T_p can be fitted as before[30] with the relation of the form

$$S = S_0 + S_{1.5}T^{1.5} + S_4 T^4, \tag{3}$$

where S_0 is a constant term having no physical origin. The low temperature (FM phase below T_p), TEP data of the samples (with $y=0.0-0.30$) are well fitted with Eq. (3) [some are shown in Figs. 9(a)–9(d)]. From the corresponding fitting parameters shown in Table V, we find $S_{1.5} \gg S_4$ which suggests that at low temperatures, S is mainly governed by the second term in Eq. (3) arising due to electron–magnon scattering contribution. It is also shown above from the low temperature (FM phase) resistivity data [Eq. (1)] that the electron–magnon scattering process dominates the conduction mechanism in the alkali metal Na-doped manganites. Therefore, from the TEP measurements also, it is reconfirmed that electron–magnon scattering process is predominant in the low temperature FM phase. Decrease of the electron–magnon scattering term ($S_{1.5}T^{1.5}$) under magnetic field suggests that spins get favorably oriented under magnetic field and hence electron-spin scattering possibility reduces and the system behaves like a metal. But in the low temperature metallic phase (below T_p), the exchange coupling strength increases leaving the electrons more delocalized and this makes the system magnetic (ferro or antiferromagnetic, depending on concentration, strength of exchange interaction). At high temperatures, the T^4 term (spin wave fluctuation contribution) cannot be neglected and this term actually fits the data [with Eq. (3)] over the high temperature region. The parameter S_0 [Eq. (3)] is found to increase in the presence of a magnetic field. However, the interdependency of the parameters S_0, $S_{3/2}$, etc. is not well known and needs further study.

Stronger support in favor of small polaron formation is obtained from the high temperature ($T > \theta_D/2$) TEP data where there is disorder and localization. In this region TEP data fits excellently with Mott's well-known equation[23] of the Seebeck coefficient based on polaron hopping, viz.,

$$S = k_B/e[E_S/k_BT + \alpha'], \tag{4}$$

where E_S is the activation energy obtained from the TEP data and α' is a constant related to the kinetic energy ($=k_BT\alpha'$) of the polarons (carriers). For $\alpha' < 1$ small polaron hopping conduction occurs, while for $\alpha' > 2$ the conduction involves large polarons.[30] Figure 10 gives the S versus $1/T$ plots for all the samples both in presence and in absence of magnetic field. Solid lines give the best fit of the experimental data with Eq. (4). From the slope of S versus $1/T$ curves, we obtain the values of activation energy E_S of the samples shown in Table III. The constant α' is obtained from the intercept of the plotted curves (Table IV). The estimated values of α' [from Eq. (4)], indicated $\alpha' < 1$ for both zero and 1.5 T magnetic field. Therefore, the small polaron hopping conduction mechanism is also strongly supported by the high temperature ($T > T_p$) TEP data. Consequently, the possibility of the formation of large polarons in $La_{0.75}Ca_{0.25}MnO_3$, as discussed by Zhao *et al.*[6] in recent papers, is not supported from the field dependent or independent TEP study for the Na/K doped samples. Zhao *et al.*[6] also used Eq. (4) for the fitting of their high temperature TEP ($T > T_p$) data. But they did not estimate α' which showed the small or bipolaron behavior in the system. From conductivity data also we have discarded the possibility of the formation of large polaron (or bipolarons) above T_p in the high temperature phase.

With the application of a magnetic field, we noticed (Table III) that the hopping energy W_H and polaron binding energy decrease, which means that the small polarons melt near the Curie temperature (in the present case around T_p since $T_p \approx T_c$). As a consequence a glasslike transition might appear near T_c depending on doping. Interestingly, a glasslike melting of polarons has been observed from recent neutron diffraction studies[31] of the La–Ca–Mn–O system. Below this glasslike transition (i.e., below T_p), as mentioned above, exchange interaction increases and electron–electron

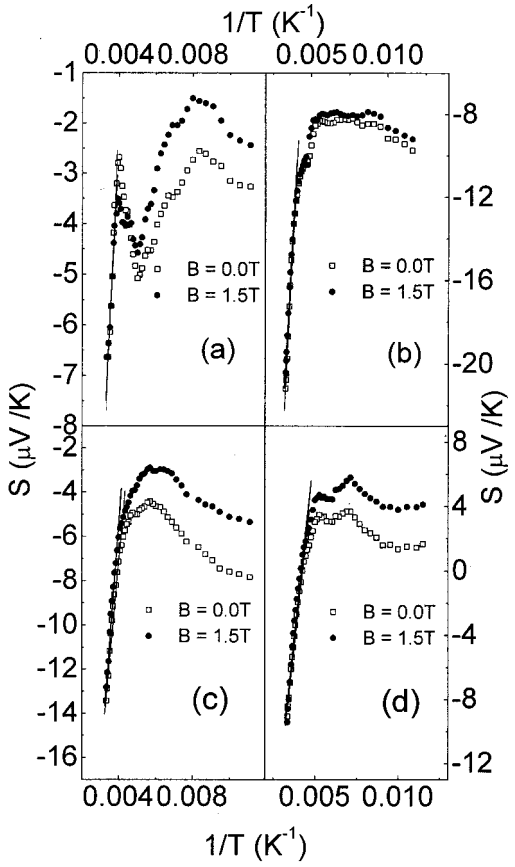

FIG. 10. The Seebeck coefficient S vs $1/T$ plot for four different $La_{0.7}Ca_{0.3-y}Na_yMnO_3$ samples with (a) $y=0.0$, (b) 0.05, (c) 0.1, and (d) 0.15. Solid lines are the best-fit lines to the Mott's model [Eq. (4)].

and electron–magnon interactions primarily draws the system to the metallic ferromagnetic state.

IV. SUMMARY AND CONCLUSION

Magnetic field dependent transport properties (resistivity and thermoelectric power) of the Na/K-doped $La_{1-x}Ca_{x-y}(Na/K)_yMnO_3$ ($x=0.3, 0.0 \leqslant y \leqslant 0.3$) system shows an increase in the dc-conductivity and metal–insulator transition temperature T_p with an increase in doping concentration (y) which is caused by the decrease of small polaron coupling constant ($\gamma=4.69-2.63$) in the high temperature ($T>T_p$) phase. Within the temperature range of our investigation, an increase of y or the increase of magnetic field (B) has the same effect on T_p and conductivity of the system studied. The high temperature ($T>T_p$) resistivity data both in the presence and in the absence of magnetic field can be fitted to the VRH model (for the regime $T_p<T<\theta_D/2$) and to the SPH model (for the regime $T>\theta_D/2$). The hopping is found to be adiabatic in nature both in presence and in absence of magnetic fields. The activation energies (E_p, E_S, W_H) and the small polaron coupling constant (γ) which is a measure of el–ph coupling strength decrease causing an increase in conductivity. The decrease of the polaron coupling constant, effective mass, binding and hopping energies mean "melting of small polarons" and the corresponding increase of conductivity. Due to high conductivity and low polaronic interaction constant, Mott's condition of strong el–ph interaction breaks above a particular Na/K doping content as a consequence the electrons get delocalized which causes an increase of conductivity. With the lowering of temperature and around T_p or T_c, where maximum electrons are delocalized (due to loss of energy by the polarons), a glasslike transition is predicted. The melting of small polarons around T_p, gives rise to the strong spin–spin (exchange) and electron–magnon interactions which is important for the creation of metallic ferromagnetic/antiferromagnetic phase (depending on y, spin–spin and electron–magnon interactions below T_p). Our results do not support the formation of large polarons (or bipolaron). High temperature TEP data also suggest the small polaron formation.

In the low temperature metallic phase, the resistivity data of the alkali metal doped manganite system are best fitted to the equation $\rho=\rho_0+\rho_2T^2$ suggesting the importance of electron–magnon scattering to be dominant in the ferromagnetic phase. The corresponding Seebeck coefficient data (in the FM phase) also well fitted to the equation $S=S_0+S_{3/2}T^{3/2}+S_4T^4$ suggesting that low temperature conduction mechanism is mainly controlled by an electron–magnon scattering process in line with the finding of conductivity measurements.

ACKNOWLEDGMENTS

The authors are grateful to the Department of Science and Technology, Government of India for financial support. One of the authors (B.K.C.) is also grateful to NSC, Taiwan (ROC) for partial financial assistance during his stay at the Department of Physics, NSYS University.

[1] A. Urushibara, Y. Moritomo, T. Arima, A. Asamitsu, G. Kido, and Y. Tokura, Phys. Rev. B **51**, 14103 (1995).
[2] R. Mahendiran, S. K. Tiwary, and A. K. Raychaudhuri, Solid State Commun. **98**, 701 (1996).
[3] C. Zener, Phys. Rev. **82**, 403 (1951).
[4] A. J. Millis, P. B. Littlewood, and B. I. Shraiman, Phys. Rev. Lett. **74**, 5144 (1995).
[5] S. Pal, A. Banerjee, E. Rozenberg, and B. K. Chaudhuri, J. Appl. Phys. **89**, 4955 (2001).
[6] Guo-meng Zhao, Y. S. Wang, D. J. Kang, W. Prellier, M. Rajeswari, H. Keller, T. Venkatesan, C. W. Chu, and R. L. Greene, Phys. Rev. B **62**, R11949 (2000); A. S. Alexandrov and A. M. Bratkovsky, Phys. Rev. Lett. **82**, 141 (1999).
[7] T. Egami and D. Louca, Phys. Rev. B **65**, 094422 (2002).
[8] M. Jaime, M. B. Salamon, M. Rubenstein, R. E. Treece, J. S. Horwitz, and D. B. Chrisey, Phys. Rev. B **54**, 11914 (1996).
[9] M. Viret, L. Ranno, and J. M. D. Coey, Phys. Rev. B **55**, 8067 (1997).
[10] A. Banerjee, S. Pal, and B. K. Chaudhuri, J. Chem. Phys. **115**, 1550 (2001).
[11] C. Boudaya, L. Laroussi, E. Dhahri, J. C. Joubert, and A. Cheikhrouhou, J. Phys.: Condens. Matter **10**, 7485 (1998).
[12] G. H. Rao, J. R. Sun, K. Bärner, and N. Hamad, J. Phys.: Condens. Matter **11**, 1523 (1999).
[13] N. Abdelmoula, A. Cheikhrouhou, and L. Reversat, J. Phys.: Condens. Matter **13**, 449 (2001).
[14] S. Roy, Y. Q. Guo, S. Venkatesh, and N. Ali, J. Phys.: Condens. Matter **13**, 9547 (2001).
[15] S. Zouari, L. Ranno, A. C. Rouhou, M. Pernet, and P. Strobel, Solid State Commun. **119**, 517 (2001).
[16] M. Jaime, P. Lin, M. B. Salamon, and P. D. Han, Phys. Rev. B **58**, R5901 (1998).
[17] S. Bhattacharya, A. Banerjee, R. K. Mukherjee, H. D. Yang, and B. K. Chaudhuri, J. Phys.: Condens. Matter **14**, 10221 (2002).

[18] N. F. Mott and I. G. Austin, Adv. Phys. **18**, 41 (1969).
[19] N. F. Mott, in *Metal–Insulator Transitions* (Taylor and Francis, London, 1974).
[20] P. Schiffer, A. P. Ramirez, W. Bao, and S. W. Cheong, Phys. Rev. Lett. **75**, 3336 (1995).
[21] G. Jeffrey Snyder, R. Hiskes, S. Dicarolis, M. R. Beasley, and T. H. Geballe, Phys. Rev. B **53**, 14434 (1996).
[22] A. J. Millis, P. B. Littlewood, and B. I. Shraiman, Phys. Rev. Lett. **74**, 5144 (1995).
[23] N. F. Mott and E. A. Davis, in *Electronics Process in NonCrystalline Materials* (Clarendon, Oxford 1971).
[24] T. Holstein, Ann. Phys. (N.Y.) **8**, 343 (1959).
[25] F. Mayr, C. Hartinger, M. Paraskevopoulos, A. Pimenov, J. Hemberger, A. Loidl, A. A. Mukhin, and A. M. Balbashov, Phys. Rev. B **62**, 15673 (2000).
[26] A. J. Millis, B. I. Shraiman, and R. Mueller, Phys. Rev. Lett. **77**, 175 (1996).
[27] D. Emin and T. Holstein, Ann. Phys. (N.Y.) **53**, 439 (1969).
[28] P. Brahma, S. Banerjee, S. Chakraborty, and D. Chakraborty, J. Appl. Phys. **88**, 6526 (2000).
[29] T. Egami and D. Louca, J. Supercond. **13**, 247 (2000); D. Louca, T. Egami, E. L. Brosha, H. Roder, and A. R. Bishop, Phys. Rev. B **56**, R8475 (1997); D. Louca and T. Egami, *ibid.* **59**, 6193 (1999).
[30] A. Banerjee, S. Pal, S. Bhattacharya, H. D. Yang, and B. K. Chaudhuri, Phys. Rev. B **64**, 104428 (2001), and references therein; S. Bhattacharya, A. Banerjee, S. Pal, R. K. Mukherjee, and B. K. Chaudhuri, J. Appl. Phys. **93**, 356 (2003).
[31] D. N. Argyriou, J. W. Lynn, R. Osborn, B. Campbell, J. F. Mitchell, U. Ruett, H. N. Bordallo, A. Wildes, and C. D. Ling, Phys. Rev. Lett. **89**, 036401 (2002).